ISSN 2321-807X

SYNTHESIS, SPECTROSCOPIC AND THERMOGRAVIMETRIC STUDIES ON SOME TRANSITION METAL COMPLEXES WITH HYDRAZONE LIGANDS.

Ahmed A. Shabana[1], Hamdy A. Hammad[1], Hassan A.Sadek[1, a],NAA Ghany[2]
Saleh D. Mekkey[1], Osama M. Yassin[3].
[1]Chemistry Department,Faculty of Science,Azhar University,Naser city,11884,Cairo ,Egypt .
Hassanelfarsy@yahoo.com.
[2]Physical chemistry, National Research centre, Dokki, 12622, Giza, Egypt.
Na_manakhly@yahoo.com
[3]Physics Department, Faculty of Science, Azhar University, Naser city, 11884, Cairo, Egypt.
Om_yassin_2030@yahoo.com

ABSTRACT

Complexes of Cu (II) and Ni (II) derived from 2-amino-N'-(2-hydroxybenzylidene) benzohydrazide**(ASH)**, 2-amino-N'-benzylidenebenzohydrazide**(ABH),** N'-(3-phenylallylidene)-2-((3-phenylallylidene)amino)benzohydrazide**(ACH),** and N'-(4-methoxybenzylidene)-2-((4-methoxybenzylidene)amino)benzohydrazide**(AAH)**have been synthesized and characterized by elemental and thermal analysis(TGA), IR, U.V-Visible, ^{1} H NMR (Ligands) spectral studies, magnetic susceptibility, atomic absorption and molar conductivity measurements, the ligand (ASH) act as tridentate with ONO donor sites, the bonding sites are carbonyl oxygen , azomethine nitrogen and phenolate oxygen, the other ligands act as bidentate with ON donor sites, the bonding sites are carbonyl oxygen, azomethine nitrogen, the metal complexes exhibit different geometrical structures such as square pyramidal,tetrahedral, square planar and octahedral. The Coats-Redfern equation has been used to calculate the thermodynamic parameters for different thermal decomposition steps of some complexes.

KEWORDS: hydrazone, transition metal complexes, coats-redfern equation, Gaussiananalysis

Council for Innovative Research

Peer Review Research Publishing System

Journal: Journal of Advances in Chemistry

Vol. 12, No. 3

editor@cirjac.com

www.cirjac.com

ISSN 2321-807X

1. INTRODUCTION

In recent years the chemistry of hydrazone has been extensively studied, owing to their coordinating capability, pharmacological activity and biological properties. The complexes of transition metals with hydrazone ligands have shown wide interest of biological and pharmaceutical activities such as antimicrobial, antibacterial, antifungal, anti-inflammatory, anticonvulsant,antibercular,antiviral, antioxidant and inhibition of tumor growth[1]–[4].The tridentate of benzhydrazone derivative ligands containing ONO donor atoms can be synthesized with any aldehyde or ketone. The presence of donor atoms in the ligands plays an important role in the formation of a stable chelate ring and this situation facilitates the complexation process[5]. The bioinorganic chemistry focused agreat attention to hydrazone complexes because many of these complexes have biologically important species[6]. In analytical chemistry hydrazone find application by act as multidentate ligands[7] with metal (usually transition metal group). Various studies have also shown that tha azomethine group having a lone pair of electrons in either a p or sp^2 hybridized orbital on trigonallyhybridized nitrogen has considerable biological importance. The hydrazone schiff's base show clearly keto-enol tautomerism and can link metal ion in neutral medium in medicinal application[8]. Thus, we are motivated to undertake a systematic study of preparation and characterization of transition metal complexes of Cu (II) and Ni (II) metal ions with some aroylhdrazone.

2. EXPERIMENTAL

2.1. Chemicals and instruments

Aldehydes were obtained from Biotech for laboratory chemicals, DMSO from Merk and all other chemicals used in the study were of reagent grade and applied without further purification.The elemental analysis were performed using CHNS-932 (LECO) Vario Elemental Analyzers, the molar conductance of complexes were measured using conductance/TDS 72 instrument. Infrared spectra were recorded on PerkinElmer FT-IR 200 spectrometer thermoelectron in 4000-400 cm^{-1}region as KBr pellets. The UV-Vis spectra were measured in the range of 200-800 nm using Perkin-Elemer Lambda 35 UV-Vis. The magnetic measurements were carried out using gouy method. The^{1}H NMR spectra were recorded in DMSO and D_2O usingGEMINI-200 NMR spectrometer. The melting point of was measured using electro thermal melting point SMPI apparatus. TGA analysis was recorded on TGA-50H in range of 25 – 1000 C°.

2.2. Synthesis of ligands

A mixture of 2-aminobenzohydrazide (0.01 mol) and substituted aromatic aldehydes (0.01 molsalicylaldhyde, 0.01 mol benzaldhyde, 0.02 mol cinnmaldhyde, 0.02 mol 4- anisaldhyde) in absolute ethanol (25ml) was heated under reflux for 1hr. this mixture was allowed tocool and the solid product was collected and recrystallized from ethanol**[9], [10].** Structures are shown in**(Fig.1)**

2.3. Synthesis of metal complexes

The complexes were prepared by the reaction Cu (II) acetate and Ni (II) acetate with ASH, ABH.Ligands in molar ratio (1:1) and with ACH and AAH ligands in molar ratio (1:2).The mixture was heated and reflux for 3hr with stirring. the product was filtered off, washed several times with ethanol and dried over anhydrous $CaCl_2$ in desiccator.[11]

2.4. Determination of metal content in complexes.

Metal complexes (5 mg) were weighted and then concentrated nitric acid (10 ml) was added. The solution was heated until few drops of the solution were remained. 10 ml deionized water was added to this hot solution, repeating this step five times then transferred the solution to a 100 ml volumetric flask. It was made up to the mark using deionized water and then the amount of metal was estimated by Atomic absorption spectroscopy**.**

3. RESULTS AND DISCUSSION

The analytical data for ligands and its complexes are given in table 1. The elemental analysis reveal that 1:1 (ligand: metal) stoichiometry for ligands ASH and ABH and 2:1 (ligand: metal) for ligands ACH and AAH. The isolated complexes are insoluble in most organic solvents but are soluble in hot DMSO.

3.1. IR spectral studies

The infrared spectra of ligands and related complexes were recorded to confirm their structures. The vibrational frequencies and their tentative assignments are listed in (Table 2). The hydrazone ligands can exist in the keto or enol forms or an equilibrium mixture of two forms since it has an amide group –NH-C=O[12] ,However the IR data indicates that in solid state the ligands is in keto-form. The IR spectrum of ASH ligand reveals a broad band at 3411 cm^{-1} attributed toν (OH) phenolic. The bands at 3322-3267 cm^{-1} due to ν (NH_2 + NH), the strong band with a shoulder noticed at 1653 cm^{-1} can be attributed to ν (C=O) [13], the spectrum also shows bands at 1600 $cm^{-1}\delta$(N-H) ,1528 cm^{-1} ν (C=N) , 874 $cm^{-1}\nu$(N–N).The IR spectra of complexes corresponding to ASH ligands reveal absence of OH band indicatingdeprotonation of the phenolic oxygen and subsequent coordination to the metal ion .This is further supported by upward shifting ofν (C–O) band by 14-41 cm^{-1}confirming the coordinating of phenolic oxygen to the metal ion[14].The disappearance of ν(C=O),ν (N–H) bands in complexes, suggests enolization of carbonyl oxygen and this is supported by appearance of

ISSN 2321-807X

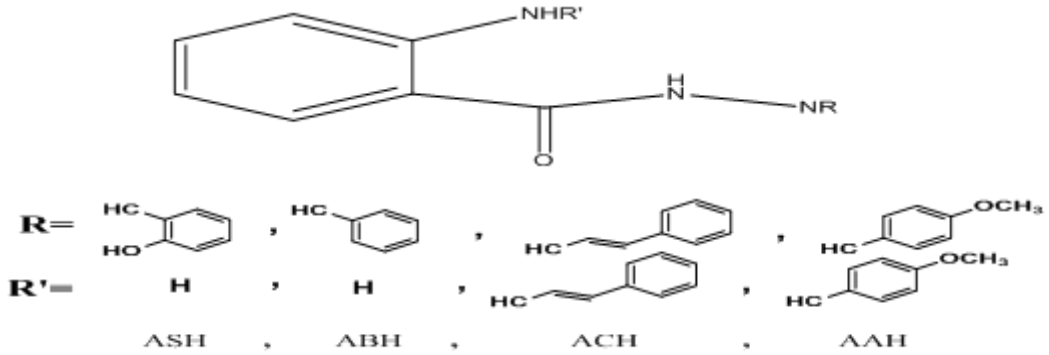

Fig 1: structures of ligands

New bands at (1369 – 1365) cm^{-1} and (540 – 542) cm^{-1} attributed to ν (C–O) enolic and ν (M–O) respectively, suggests the coordination of carbonyl oxygen to the metal ion after deprotonating. The band ofν(C=N) in ligand is found to be shifted to lower frequency by 19-28 cm^{-1} indicating the coordination via the Azomethine nitrogen [15], which also is confirmed by appearance of bands in the range of 437–443 cm^{-1} which have been assigned to ν (M–N). The (N–N) band in ligand is shifted to higher frequency in complexes at 890 – 896 $cm^{-1}$and this frequency shift supported the coordination through azomethine nitrogen[16]. The complexes also show newbands at 3380 and 3426 cm^{-1} attributed to the presence of water molecules. The IR spectrum of ABH ligand indicates the observation of ν (NH_2) vibrations as doublet at 3488 -3376 cm^{-1}, the ν (N–H) band of hydrazine moiety appears at 3210 cm^{-1}, the band observed at 1634 cm^{-1} is assigned to carbonyl group, the bands at 1541 and 1250 $cm^{-1}$is attributed to (ν C=N,δ N–H) and amide III respectively. By comparing the IR spectra of complexes with that of ABH ligand, it can be deduced that enolization of carbonyl oxygen and subsequent coordination to the metal ion through the oxygen after deprotonation ,this is supported by disappearance of ν (N–H) band of hydrazinemoiety and appearance a new bands at (1367– 1365) cm^{-1} and (597 – 620) cm^{-1} due to ν (C–O) enolic and ν (M–O) respectively, and also the band of azomethine group in free ligand is shifted to lower frequency by 29- 35 cm^{-1}, the band in free ligand at 967 cm^{-1} is shifted to higher frequency in complexes at 1034 and 1018 cm^{-1} due to ν (N–N) suggesting the coordination through azomethine nitrogen and is supported by appearance of new band at (452 – 432)cm^{-1} due to ν (M–N). The observed New bands in range of 1590 – 1598 cm^{-1} and 1445 – 1446 cm^{-1}range are assigned to ν_{as} and $\nu_s(COO^-)$ referring to the coordinating acetate, which coordinate as bidentate ligand. The IR spectraof ACH ligand showed bands at 3256, 1628, 1515, 1395 and 967 cm^{-1}assigned to ν (N–H), ν (C=O), (ν C=N+ δ N-H), amide III and ν (N–N) respectively. The IR spectra of the complexes of ACH ligands show carbonyl group shifted to lower frequency by 22-26 cm^{-1} suggesting that ligand attached to metal through carbonyl group and this is further supported by the appearance of new band in the range of 421 - 447 cm^{-1} due to (M–O) , also the lower shift of ν(C=N) band suggested that the azomethine nitrogen acts as donor site , this is further supported by shifting of ν(N–N) band to higher frequency and appearance of new band due to ν (M–N) at 519 and 521 cm^{-1}, also the bands at (1500, 1501) cm^{-1} and (1444, 1442) cm^{-1} may be due toν_{as} and ν_s (COO^-), The new bands observed at 3404 and 3438 cm^{-1} are assigned to water molecules. The most significant IR bands of AAH ligand are observed at 3338, 1626, 1522, 1357, 1247 and 902 cm^{-1} assigned to ν(N–H), ν (C=O), ν (C=N)+ δ (N–H), ν (C–O–C), amide III and ν (N–N) respectively. The IR spectra of complexes show that the carbonyl band is shifted to lower frequency by comparing with that of ligand, the shift indicates coordination of carbonyl oxygen to metal ion and also supported by appearance of new bands at 447 and 485 cm^{-1} due to ν (M–O). The stretching frequency of ν(C=N) shifted to lower frequency at 1500 and 1507 cm^{-1} andν (N–N) is shifted to higher frequency at 919 and 904 cm^{-1}, thereby suggests participation of azomethine nitrogen, the bands at 1500-1507 and 1445-1436 cm^{-1} is attributed to ν_{as} and ν_s (COO^-), and also band at 3444 -3430 $cm^{-1}$is assigned to water molecules.

3.2. ^{1}H NMR spectroscopy

The assignment of the main signals in the ^{1}H NMR spectra of the ligands are given in (table 3), ^{1}H NMR spectra of ligands exhibited multiple signals of the aromatic protons in the range of 6.5–8.5 ppm, the δ N-H proton appears in ASH, ABH, ACH and AAH at 11.449, 11.527, 7.481 and 7.625 ppm respectively, the spectrum of ASH**(Fig 2)** exhibits a signal at δ 11.849 assigned to OH proton, the signal at 6.441 and 6.309 ppm in the spectrum of ASH and ABH is assigned to NH_2

proton respectively, the disappearance of OH, NH, NH_2 protons is confirmed after the addition of D_2O. The (CH=N) proton appears as singlet at 8.568, 8.391, 8.749 ppm in ASH, ABH and AAH respectively while the (CH=N) proton in ACH ligand appears as a doublet at 8.7 ppm.

3.3. Conductivity measurement

The molar conductance$\Lambda_M$values of metal complexes in DMSO (10^{-3} M solution) were measured at room temperature and the results are listed in (table 4).it is concluded from the results that metal complexes **1, 2, 3** and **4** were found to have molar conductance values in range of 10 – 35 Ω^{-1} cm^2 mol^{-1} indicating that they are not electrolytic in nature and there is no counter ion present outside their coordination sphere**[17].**On the other hand, the molar conductivity values of

complexes 5-8 were found to have molar conductance values in the range of 99 – 145 Ω^{-1} cm^2 mol^{-1}indicating the ionic properties of these complexes.

3.4. Electronic spectra and magnetic susceptibility

The assignment of the observed electronic absorption bands of the transition metalcomplexes as well as the geometry and magnetic data of the complexes are shown in (Table 4).The ligands have spectral bands in the range of 39,682– 27,100 cm^{-1} corresponding to $\pi\pi^*$ and$n \longrightarrow \pi^*$transition in DMSO solvent.

In ASH complexes: the electronic spectrum of Cu complexshows abroad band at 15432 cm^{-1} corresponding to d–d transition characteristic of square pyramidal distorted structure of Cu (II) complex[18], [19], this band has been resolved to combination of four Gaussian functions**(Fig 3a)**. According to previousreported experimental and theoretical data of Cu (II) compounds , the Gaussian function expected for square pyramidal structure, would be three peaks corresponding tod_{z^2} $d_{x^2-y^2}$, d_{xy} $d_{x^2-y^2}$ and $d_{xz,}$ d_{yz} $d_{x^2-y^2}$ transitions[20]**.** The four Gaussian functions are attributed to the low symmetry around of Cu (II), four oxygen and one nitrogenatoms. In addition to the nitrogen apical atom shows a deviation of its perpendicularity to the square pyramidal base whichestablishes an interaction between electronic density of the nitrogen ligand and some of the atomic orbitals $d_{xz}$and d_{yz}, promoting a minimum differentiation between both d atomic orbitals (**fig 3b).**the magnetic moment μ_{eff} =2.02 B.M. which confirms the square pyramidal structure[21]**.** The electronic spectrum of Ni (II) complex (2) shows two absorption bands at 24390 and 18762 cm^{-1} characteristic of high spin five coordinated Ni (II) complex and could be assigned to $^3B_{1g}$ $^3A_{2g}$(p) and $^3B_{1g}$ ^3E_g (p) respectively of square pyramidal environment with D_{4h}symmetry [22], the magnetic moment μ_{eff} =2.86 B.M.is consistent with square pyramidal geometry.

In ABH complexes: The copper (II) complex shows a band at 17544 cm^{-1} which corresponding to the transition of the$^2T_2$ $^2E_2$consistent with distorted tetrahedral geometry[23], this is supported by magnetic moment μ_{eff} =1.83 B.M. The magnetic moment value of Ni (II) complex is 3.36 B.M., suggesting the presence of two unpaired electrons that reveals the spin free nature of the complex corresponding to tetrahedral geometry. The nickel complex shows bands at 19493 and 27624 cm^{-1} due to $^3T_{1g}$ (F) $^3T_1$(p) and $^3T_1$(F) $^3A_2$(F) transition indicating tetrahedral geometry[24]**.**

In ACH and AAH complexes: The electronic spectra of the copper (II) complexes showed d-d broad bands at 15873 and 16528 cm^{-1}respectively **which** can be assigned to ^2E_g $^2T_{2g}$transitionof an octahedral geometry.Though, in cases where the ^2E_g and $^2T_{2g}$ states of the octahedral Cu (II) ion (d^9)split under the influence of the tetragonal distortion, three transitions$^2B_{1g}$ ^2E_g, $^2B_{1g}$ $^2B_{2g}$, and $^2B_{1g}$ $^2A_{1g}$are expected , their very close energies could have made them appear in the form of one broad band envelope. Our results are in good agreement with those reported for a distorted octahedral geometry around Cu (II) ion[25]. The magnetic moment values (1.62 and 1.71 B.M. respectively) are in agreement with an octahedral geometry. The electronic spectra of Ni (II) complexesdisplay only two bands at (16234 – 24390) and (14265 – 16447) cm^{-1}, which are attributed to $^3A_{2g}$(F) $^3T_{1g}$(F) (ν_2)and $^3A_{2g}$(F) $^3T_{1g}$(p)(ν_3)transitions, respectively indicating an octahedral nickel(II) complex. The values of magnetic moment for nickel(II) complexes are 2.80 and 2.87 respectively which is consistent with two unpaired electrons state confirming octahedral geometry for nickel(II)[26], [27]**.**

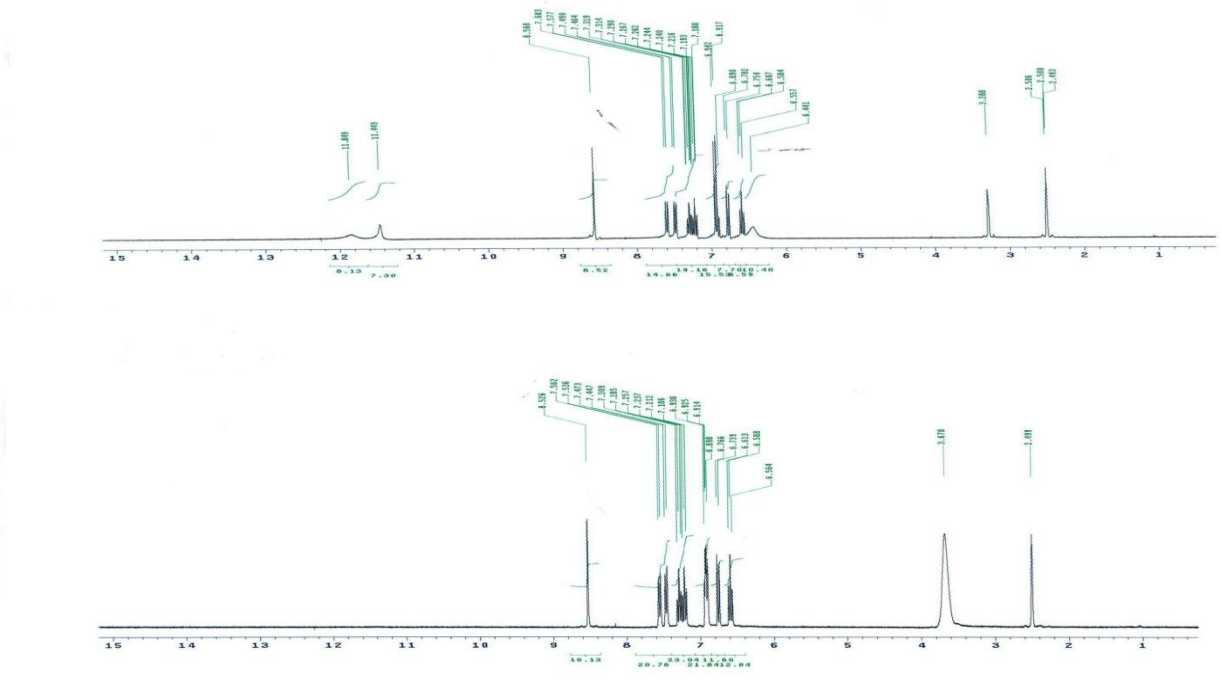

ISSN 2321-807X

Fig 2: ^{1}H NMR spectra in DMSO-d_6 solvent of the (a) ASH ligand and (b) ASH ligand after the addition of D_2O

3.5. Thermogravimetric analyses

The thermogravimetric of complexes were recorded in the temperature range 25–1000 C°(**Fig 4**). Thethermogravimetric data are given in (table 5). The thermal decomposition process of complex **1**involves three decomposition steps; the first step in the decomposition is started at 99–220 C° corresponding to loss of two coordinated water molecules (weight loss; calc./found%; 5.37/5.89), the second step in the range 221–338C°corresponding to loss of species molecules(2HCN and 2CN) with weight loss (calc./found%;15.80/15.10) , while the third step in range 338–529 C° which is attributed to the loss of fragment ($C_{24}H_{20}N_2O_2$) with weight loss (calc./found; 54.90/54.42) leaving cupper oxides 2CuO as final residue (calc/found; 23.74/24.59).The TG curve of the complex**2** reveals that the decomposition takes place in two steps. The first one at 74–163C° corresponds to a weight loss of (calc/found%; 5.44/4.76%) and is probably due to decomposition of the twocoordinated water, the second stage of decomposition takes place at 236–571.2 C°Corresponding to the organic moiety of complex with weight loss (calc. /found%; 76.76/76.56) leavening the nickel metal **2Ni** as final residue (calc./found%;17.79/17.73). The thermogravimetric analysis of complex **3** reveals two steps of decomposition, the first step started in range of 211–236 C°corresponding to fragments (acetate group, N_2, HCN and phenyl ring) with weight loss (calc. /found %; 52.98/52.24), the second step takes place at 292–336 C°which is attributed to propane species (weight loss; calc. /found %;11.64/12.88), the residue of decomposition is **CuO + 4C**(Calc/found%; 35.33/34.88). thedecomposition of complex **4** shows two stages, the first step in the range of 183 – 353 C° and is attributed to elimination of CH_3COO^-, $2C_2H_2$ and CN with weight loss (calc. / found%; 38.5/37.62%), the second step started at 353 C° and ended at 449 C°indicating loss of benzene ring and 2HCN with weight loss (calc. /found%; 38.2/39.3%),the final residue is found to be **NiO + 4C**(calc. /found; 24.40/23.08). the TGA curve of complex **5** isindicating four steps. The temperature range 42– 183 C°corresponding to the loss of lattice water, two acetate group, CO

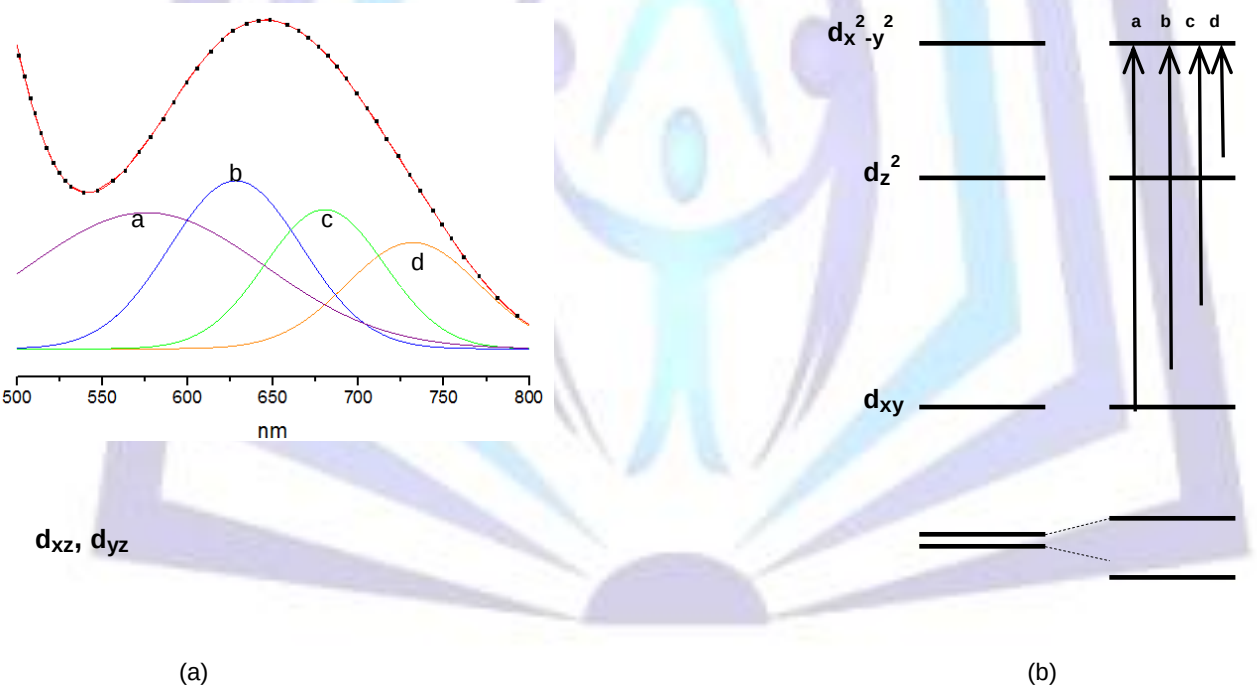

Figure 3: (a) Electronic spectrum in visible region of complex 1. Experimental (....), adjusted by Gaussian curves and their sum (—) , (b) proposed d-d transition in low symmetry atomic d orbitals.

and NH fragments (calc. /found; 17.99/18.10).The second step (183–237C°) indicates the loss of two coordinated water, 5HCN and $3C_2H_2$(calc. /found; 25.04/25.53%), the third peak appeared in the range 237–317 C°is assigned to elimination of$2C_2H_2$, phenyl ring and C_6H_4 with weight loss (calc. /found %; 20.61/19.15%). The last step refers to loss of C_2H_2 and 3 phenyl ring groups (calc. /found; 25.8/26.6) leaving **CuO + 2C**(calc. /found; 10.41/10.65). the complex **6** shows three stages, the first stage in the range of30 -119 C° and is assigned to loss of 3 lattice water molecules (calc. /found;5.26/5.73%), the second step (120 – 303 C°) indicates elimination of two coordinated water and two acetate groups (calc. /found;15.01/14.37). the final step in rang of 307 – 374 C°referring to weight loss of 67.10% (calc. 66.59%) which is due to the organic part of complex leaving **NiO + 5C** as residual form (calc./found%; 13.13/12.89%). The TGA studies of the complex **7** involve two steps, the first step in range of (170–383C°)corresponding to loss of two coordinated water, two acetate group, CO, $2C_6H_4$and 2 C_7H_7O with weight loss (calc./found%;55.50/55.70%), the second step at 295 – 456 C°

ISSN 2321-807X

involves loss of 2HCN, 2NH and $C_8H_8ON_2$ (calc./found%;35.64/35.53%) and the final residue is attributed to **NiO + C** (calc. /found%;8.76/8.77%).

3.5.1 Calculation of thermodynamic parameter of complexes

the thermodynamicparameter for thermal decomposition steps of complexes have been studied employing the Coats–Redfern equation in the following form [28]**.**

$$\log\left[\frac{1-(1-\alpha)^{1-n}}{T^2(1-n)}\right] = \log\frac{AR}{\Theta E^*}\left[1-\frac{2RT}{E^*}\right] - \frac{E^*}{2.303RT} \quad n \neq 1 \quad (1)$$

$$\log\left[\frac{-\log(1-\alpha)}{T^2}\right] = \log\frac{AR}{\Theta E^*}\left[1-\frac{2RT}{E^*}\right] - \frac{E^*}{2.303RT} \quad n = 1 \quad (2)$$

Where E*, R, A and θ are the energy of activation, the universal gas constant, pre-exponential factor and the heating rate, respectively. The correlation coefficient, R^2, was computed using the least square method by plotting the left-hand side of equation 1 or 2 vs 1000/T **(Fig 5)**. The n value which give the best fit ($R^2 \approx 1$) was chosen as the order of the parameter for the decomposition stage. From the intercept and linear slop of such stages, the A and E* values were determined. The values of activation enthalpy (ΔH*), the activation entropy (ΔS*) and the free energy of activation (ΔG*) given in (Table 6) were calculated using equation (3), (4) and (5). Where the A, k, and h are the pre-exponential factor, Boltzmann and plank's constant. The negative values of activation entropy (ΔS*) indicated that the reactions are slow and the products are more stable than reactants and the positive values of (ΔS*) indicated that the activated complexes for the decomposition stage has a less ordered structure compared to the reactant, further the reaction may be described as faster than normal.

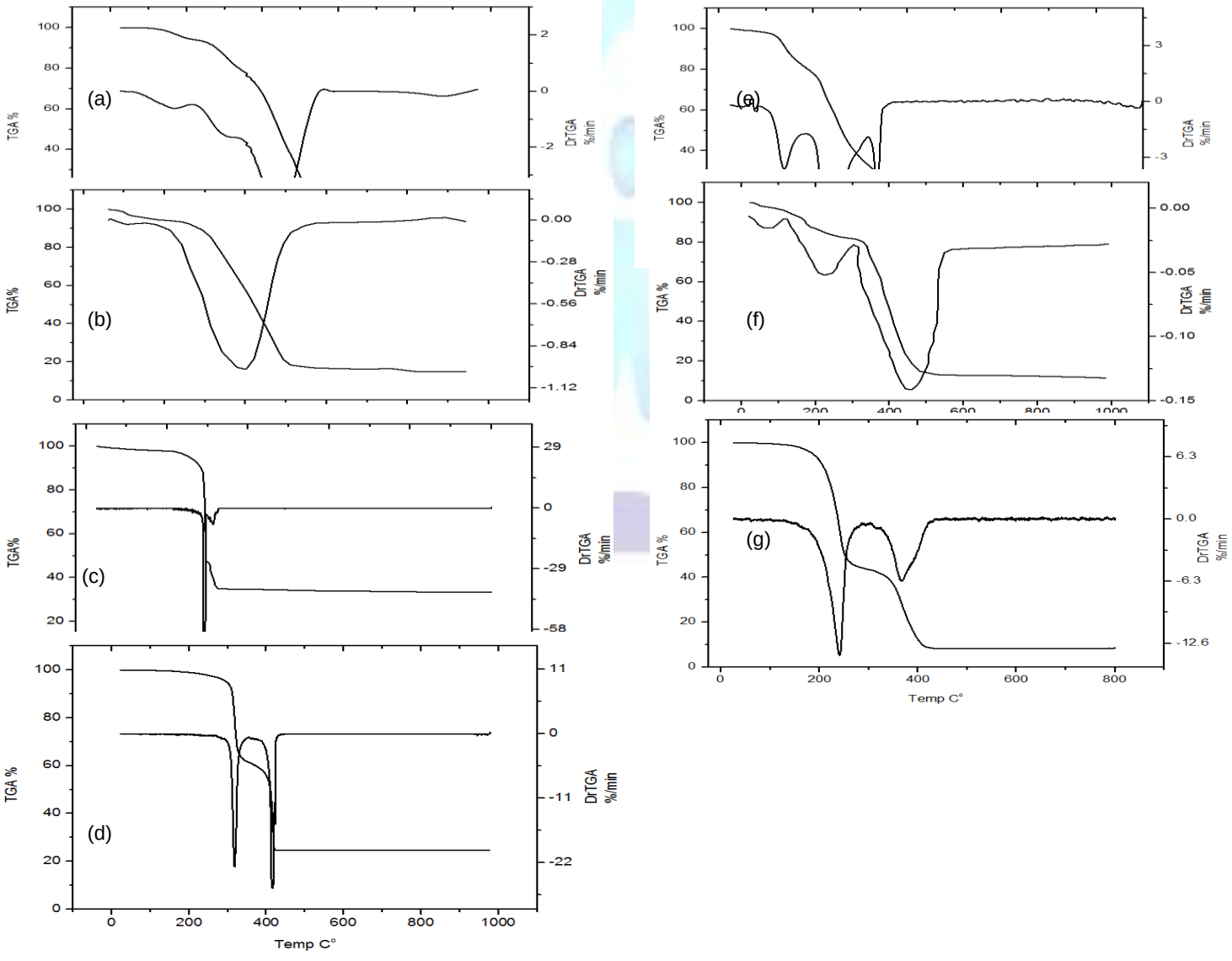

ISSN 2321-807X

Fig 4: TGA and DrTGA curve of complexes 1, 2, 3, 4, 5, 6 and 7

The positive values of enthalpy (ΔH*) mean that the decomposition processes are endothermic. The values of (ΔG*) increase significantly for the subsequently decomposition stages, increasing the values of (ΔG*) as going from one decomposition step subsequently to another reflects that the rate of removal of the subsequent ligand will be lower than that of the precedent ligand and the reactions are non-spontaneous.

$$\Delta H^* = E^* - RT \quad (3)$$

$$\Delta S^* = 2.303 \left(\log \frac{Ah}{kT}\right) R \quad (4)$$

$$\Delta G^* = H^* - TS^* \quad (5)$$

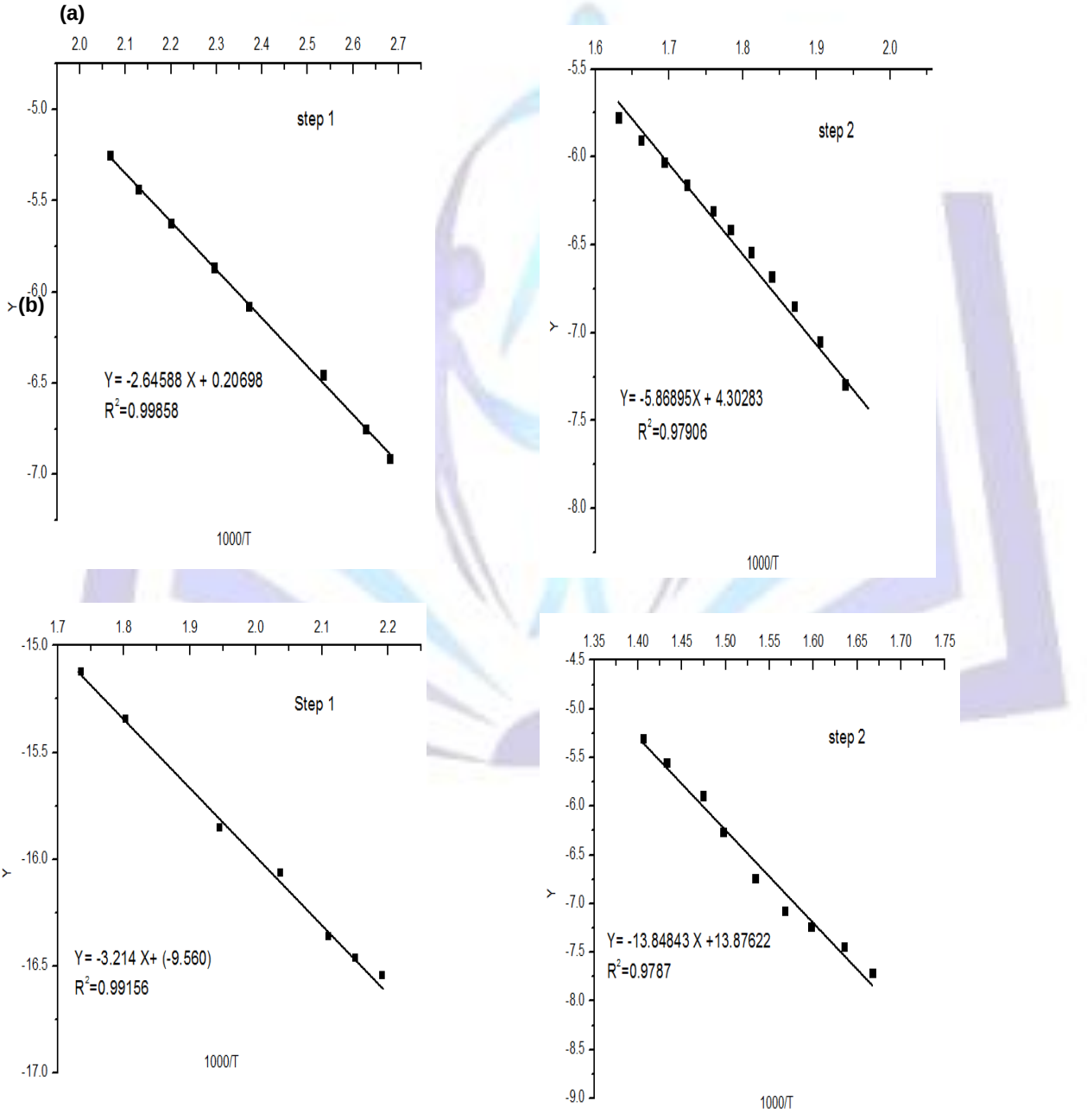

ISSN 2321-807X

Fig 5: (a)Coats-Redfern plots for complex (1) $[(Cu)_2(ASH)_2(H_2O)_2]$, (b) Coats-Redfern plots for complex (3) [Ni(ABH)(OAC)] where $Y = \ln[-\ln(1-\alpha)/T^2]$ **at** $n = 1$, **or** $Y = \ln[1-(1-\alpha)^{1-n}/T^2(1-n)]$ $n \neq 1$ **and X= 1000/T**

Table 1: Physicochemical properties of ligands and their tramnsition metal complexes

	Ligands/complexes	M.F.	M.wt.	Y%	Colour	M.P.	Elemental analyses found (calc.)			
							C%	H%	N%	M%
I	ASH	$C_{14}H_{13}N_3O_2$	255	68.7	pale yellow	166	65.12 (65.87)	4.90 (5.13)	16.20 (16.46)	–
II	ABH	$C_{14}H_{13}N_3O$	239	71.8	white	200	70.50 (70.28)	5.31 (5.48)	17.76 (17.56)	–
III	ACH	$C_{25}H_{21}N_3O$	379.4	81.9	yellow	203	78.80 (79.13)	5.10 (5.58)	10.70 (11.01)	–
IV	AAH	$C_{23}H_{21}N_3O_3$	387.4	79.5	white	161	70.60 (71.30)	5.11 (5.46)	10.28 (10.85)	–
1	$[Cu_2(ASH)_2(H_2O)_2]$	$C_{28}H_{26}N_6O_6Cu_2$	669.69	59.2	green	>300	50.53 (50.22)	4.20 (3.91)	12.69 (12.55)	18.00 (19.98)
2	$[Ni_2(ASH)_2(H_2O)_2]$	$C_{28}H_{26}N_6O_6Ni_2$	659.93	66.4	dark yellow	>300	50.63 (50.96)	3.55 (3.97)	12.34 (12.73)	18.10 (17.79)
3	[Cu(ABH)(OAC)]	$C_{16}H_{15}N_3O_3Cu$	360.8	63.5	brown	>300	52.88 (53.25)	4.64 (4.19)	12.20 (11.64)	18.30 (17.61)
4	[Ni(ABH)(OAC)]	$C_{16}H_{15}N_3O_3Ni$	356	76.5	yellow	>300	54.00 (53.98)	4.64 (4.25)	12.30 (11.80)	15.80 (16.49)
5	$[Cu(ACH)_2(H_2O)_2].(OAC)_2.H_2O$	$C_{54}H_{54}N_6O_9Cu$	994.6	81.6	dark brown	>300	64.80 (65.21)	5.02 (5.47)	7.90 (8.45)	6.80 (6.39)
6	$[Ni(ACH)_2(H_2O)_2].(OAC)_2.3H_2O$	$C_{54}H_{58}N_6O_{11}Ni$	1025.8	78.6	yellow	>300	63.17 (63.23)	4.60 (5.70)	9.28 (8.19)	5.25 (5.72)
7	$[Cu(AAH)_2(H_2O)_2].(OAC)_2$	$C_{50}H_{52}N_6O_{12}Cu$	992.5	66.2	brown	215	61.06 (60.5)	4.50 (5.28)	9.52 (8.47)	6.05 (6.40)
8	$[Ni(AAH)_2(H_2O)_2].(OAC)_2$	$C_{50}H_{52}N_6O_{12}Cu$	987.7	61.6	yellow	280	61.19 (60.80)	4.75 (5.31)	9.32 (8.51)	6.32 (5.94)

ISSN 2321-807X

Table 2: IR frequencies of characteristic bands of ligands and their metal complexes

Comp. No. / ligands	ν(OH) phenolic/H_2O	ν(NH_2)	ν(N-H)	ν(C=O)	ν(C=N)	Amide III	$\nu_{as}(COO^-)$	$\nu_s(COO^-)$	ν(C-O) enolic	ν(N-N)	ν(M-O)	ν(M-N)
ASH	3411	3322-3267	3267	1653	1528	1255	–	–	–	847	–	–
[1]	3380	3328-3228	–	–	1500	–	–	–	1369	890	542	443
[2]	3426	3314-3245	–	–	1509	–	–	–	1365	896	540	437
ABH	–	3488-3376	3210	1634	1541	1250	–	–	–	967	–	–
[3]	–	3412-3306	–	–	1506	–	1590	1445	–	1034	597	452
[4]	–	3436-3342	–	–	1512	–	1598	1446	–	1018	620	432
ACH	–	–	3256	1628	1515	1395	–	–	–	967	–	–
[5]	3404	–	3252	1602	1500	1375	1500	1442	–	985	521	447
[6]	3438	–	3287	1606	1501	1370	1501	1444	–	995	519	421
AAH	–	–	3338	1626	1522	1247	–	–	–	902	–	–
[7]	3430	–	3331	1618	1507	1249	1507	1436	–	904	534	486
[8]	3444	–	3338	1604	1500	1248	1500	1445	–	920	535	447

ISSN 2321-807X

Table 3: ^{1}H NMR chemical shifts (δ, ppm) of ligands

Ligand	δ(CH=N)	δ(N-H)	δ(Ph-proton)	δ(NH_2)	δ(OH)
ASH	8.6 (s, 1H)	11.4 (s, 1H)	6.5 - 7.6 (m, 8H)	6.4 (S, 2H)	11.8 (S, 1H)
ABH	8.4 (S, 1H)	11.5 (S, 1H)	6.5 - 7.7 (m, 9H)	6.3 (S, 2H)	_
ACH	8.7 (d, 2H)	7.4 (S, 1H)	6.9 - 7.7 (m, 14H)	_	_
AAH	8.7 (S, 2H)	7.6 (S, 1H)	6.3 - 7.7 (m, 12H)	_	_

Table 4: Electronic absorption bands, magnetic moments and molar conductivity of metal complexes

Comp. No.	d-d transition (cm^{-1})	d-d transition assignment	$\mu_{eff.}$ (B.M.)	Λ (Ω^{-1} cm^2 mol^{-1})	Geometry structure
[1]	15432	$^{2}E_g \longrightarrow {}^{2}T_{2g}$	2.02	14	square pyrmidal
[2]	18762	$^{3}B_{1g} \longrightarrow {}^{3}E_g(p)$	2.86	26	square pyrmidal
	24390	$^{3}B_{1g} \longrightarrow {}^{3}A_{2g}(p)$			
[3]	17544	$^{2}T_2 \longrightarrow {}^{2}E$	1.83	10	tetrahedral
[4]	19493	$^{3}T_1(F) \longrightarrow {}^{3}T_1(P)$	3.36	29	tetrahedral
	27624	$^{3}T_1(F) \longrightarrow {}^{3}A_2(F)$			
[5]	15873	$^{2}E_g \longrightarrow {}^{2}T_{2g}$	1.62	99	octahedral
[6]	16234	$^{3}A_{2g}(F) \longrightarrow {}^{3}T_{1g}(F)$	2.8	137	octahedral
	24390	$^{3}A_{2g}(F) \longrightarrow {}^{3}T_{1g}(P)$			
[7]	16528	$^{2}E_g \longrightarrow {}^{2}T_{2g}$	1.71	145	octahedral
[8]	14265	$^{3}A_{2g}(F) \longrightarrow {}^{3}T_{1g}(F)$	2.87	129	octahedral
	16447	$^{3}A_{2g}(F) \longrightarrow {}^{3}T_{1g}(P)$			

ISSN 2321-807X

Table 5: Thermogravimetric analysis data of metal complexes

Comp. No.	DTG $_{max}$ (C°)	Temp. range	eliminated species	%mass loss found (calc.)	Metallic residual % found (calc.)
[1]	167	99 - 220	$2H_2O$ (coord.)	5.89 (5.37)	2CuO 24.59 (23.74)
	320	220 - 338	2HCN and 2CN	15.10 (15.80)	
	449	338 - 529	$C_{24}H_{20}N_2O_2$	54.42 (54.90)	
[2]	108	74 - 163	$2H_2O$ (coord.)	4.76 (5.44)	2Ni 17.73 (17.79)
	401	236 - 571	the remaining of ligand	76.56 (76.76)	
[3]	290	211 -293	CH_3COO^-,N_2, HCN and C_6H_5	52.24 (52.98)	CuO + 4C 34.88 (35.33)
	313	292 - 336	C_3H_8	12.88 (11.64)	
[4]	317	183 - 353	CH_3COO^-, $2C_2H_2$ and CN	37.62 (38.50)	NiO + 4C 23.08 (24.4)
	416	353 - 449	C_6H_6 and 2HCN	39.30 (38.2)	
[5]	139	42 - 183	H_2O (hydr.), $2CH_3COO^-$, CO and NH	18.10 (17.99)	CuO + 2C 10.65 (10.41)
	220	183 - 237	$2H_2O$ (coord.), 5HCN and $3C_2H_2$	25.53 (25.04)	
	253	237 - 317	$2C_2H_2$,C_6H_5 and C_6H_4	19.15 (20.61)	
	336	317 - 374	C_2H_2 and $3C_6H_5$	26.60 (25.80)	
[6]	70	30 - 119	$3H_2O$ (hydr.)	5.73 (5.26)	NiO + 5C 12.89 (13.13)
	225	120 - 303	$2H_2O$ (coord.) and $2CH_3COO^-$	14.37 (15.01)	
	455	307 - 594	the remaining of organic moiety	67.10 (66.59)	
[7]	241	102 - 295	$2H_2O$ (coord.), $2CH_3COO^-$, CO, $2C_6H_4$ and $2C_7H_7O$	55.70 (55.5)	NiO + C 8.77 (8.76)
	368	295 - 456	2HCN, 2NH and $C_8H_8ON_2$	35.53 (35.64)	

Table 6: Thermodynamic data of thermal decomposition of metal complexes

Comp. no.	complex	Step	DTG$_{max}$ (k)	log A (S^{-1})	ΔE* (KJ mol^{-1})	ΔH* (KJ mol^{-1})	ΔS* (KJ $mol^{-1}K^{-1}$)	ΔG* (KJ mol^{-1})
1	$[(Cu)_2(ASH)_2(H_2O)_2]$	1st	440.20	4.99	50.70	47.03	-0.15	114.20
		2nd	593.30	9.43	112.50	107.50	-0.07	149.10
		3rd	721.80	7.14	112.30	106.30	-0.12	189.80
2	$[(Ni)_2(ASH)_2(H_2O)_2]$	1st	381.30	6.31	53.10	49.90	-0.13	97.90
		2nd	674.40	1.04	33.40	27.80	-0.23	184.10
3	[Cu(ABH)(OAC)]	1st	562.60	1.98	39.10	34.40	-0.21	153.90
		2nd	586.40	17.70	201.20	196.30	0.09	143.90
4	[Ni(ABH)(OAC)]	1st	590.30	0.36	26.70	21.80	-0.24	165.70
		2nd	689.10	19.40	265.30	259.60	0.11	177.50
5	$[Cu(ACH)_2(H_2O)_2].(OAC)_2.H_2O$	1st	411.60	1.74	27.40	23.99	-0.21	112.20
		2nd	492.90	16.10	157.60	153.50	0.06	124.10
		3rd	552.70	13.55	143.80	139.20	0.01	134.02
		4th	608.90	35.46	416.70	411.60	0.43	151.00
6	$[Ni(ACH)_2(H_2O)_2].(OAC)_2.3H_2O$	1st	343.20	4.78	52.60	49.80	-0.16	102.90
		2nd	498.10	4.82	52.90	48.80	-0.16	126.95
		3rd	727.90	4.84	79.50	73.40	-0.16	189.70
7	$[Ni(AAH)_2(H_2O)_2].(OAC)_2$	1st	514.00	8.28	88.19	83.90	-0.09	130.60
		2nd	641.10	10.20	137.40	132.10	-0.06	168.33

ISSN 2321-807X

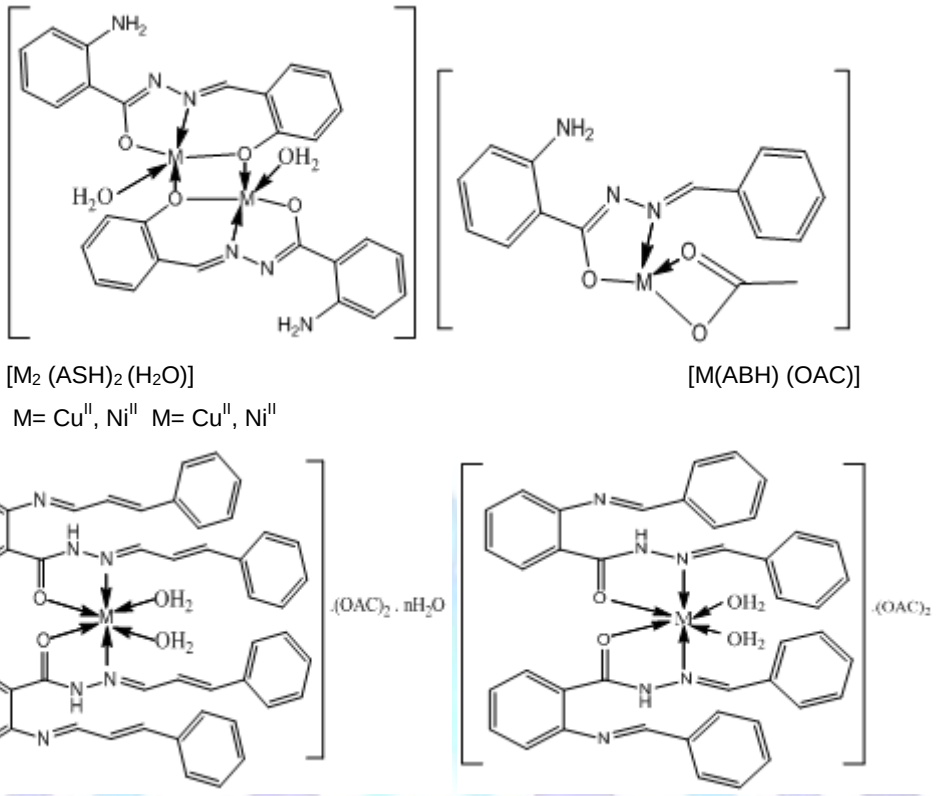

$[M_2 (ASH)_2 (H_2O)]$ $[M(ABH) (OAC)]$

M= Cu^{II}, Ni^{II} M= Cu^{II}, Ni^{II}

$[M (ACH)_2(H_2O)_2].(OAC)_2.n(H_2O)$ $[M (AAH)_2 (H_2O)_2].(OAC)$

M= Cu^{II}, n= 1 M= Cu^{II}, Ni^{II}

Ni^{II}, n= 3

Fig. 6: Proposed structure of metal complexes

4. CONCLUSION

From the elemental analysis, IR and UV-Vis spectral data, molar conductivity and magnetic measurements and thermogravimetric analyses, it can be concluded that the ligands appearin keto-form and behave as bidentate (ABH, ACH and AAH) or tridentate (ASH) forming square pyramidal for ASH, tetrahedral for ABH and octahedral geometry for ACH and AAH complexes, the thermodynamic data of decomposition processes of complexes were calculated by employing the Coats – Redfern equation.

REFERENCE

[1] "Ahmed A. El-Sherif," *Inorganica Chim. Acta*, vol. 362, pp. 4991–5000, 2009.

[2] "Madalina Veronica Angelusiu,Stefania-felicia Barbuceanu, Constantin Draghici, Gabriela Laura Almajan," *Eur. J. Med. Chem.*, vol. 45, pp. 2055–2062, 2010.

[3] "K. Kashinath, Vijaykumar Durg, KalpanaBaburao and SD. Angadi," *Int. J. Res. Pharm. Chem.*, vol. 4, pp. 557–563, 2014.

[4] "Paweł Subik, Agata Białońska, Stanisław Wołowiec," *Polyhedron*, vol. 30, pp. 873–879, 2011.

[5] "Antonio Sousa-Pedrares, Nuria Camiña, Jaime Romero, Maria L. Durán, José A. García-Vázquez, Antonio Sousa," *Polyhedron*, vol. 27, pp. 3391–3397, 2008.

[6] "Mostafa El-Behery, Haifaa El-Twigry," *Spectrochim. Acta - Part A Mol. Biomol. Spectrosc.*, vol. 66, pp. 28–36, 2007.

[7] "Yoshiya Ikawa, Toshi Nagata, Kazuhiro Maruyama," *Chem. Lett.*, vol. 22, pp. 1049–1052, 1993.

[8] "G.M.Dongare, R.T.Parihar," *J. Med. Chem. drug Discov.*, pp. 484–488, 2013.

[9] "Hassan, Dheefaf F," *J. Al-Nahrain Univ.*, vol. 13, pp. 32–39, 2010.

[10] "Bharat Parashar , P. B. Punjabi , G. D. Gupta and V. K. Sharma," *Int. J. ChemTech Res.*, vol. 1, pp. 1022–1025, 2009.

[11] "Azza A.A. Abu-Hussen, Wolfgang Linert," *Spectrochim. Acta. A. Mol. Biomol. Spectrosc.*, vol. 74, pp. 214–223, 2009.

[12] "Amina A.Soayed, Heba M. Refaat, Leena Sinha," *J. Saudi Chem. Soc.*, vol. 19, pp. 217–226, 2014.

[13] "N. Kavitha, P.V. Anantha Lakshmi," *J. Saudi Chem. Soc.*, vol. 19, pp. 575–579, 2015.

[14] "Ravindra Bhaskar, Nilesh Salunkhe, Amit Yaul, Anand Aswar," *Spectrochim. ACTA Part A Mol. Biomol. Spectrosc.*, vol. 151, pp. 621–627, 2015.

[15] "S. R. Kelode, T. R. Kale, P. R. Mandlik," *Int. J. ChemTech Res.*, vol. 5, pp. 362–366, 2013.

[16] "O.Sunita Devi, Ak. Manihar Singh," *J. Chem. Pharm. Res.*, vol. 3, pp. 1055–1060, 2011.

[17] "Abeer A. Faheim, Safaa N. Abdou, Zeinab H. Abd El-Wahab," *Spectrochim. Acta. A. Mol. Biomol. Spectrosc.*, vol. 105, pp. 109–124, 2013.

[18] "Yasmi Reyes-Ortega, José Luis Alcántara-Flores, María del Carmen Hernández-Galindo, René Gutiérrez-Pérez, Daniel Ramírez-Rosales, Sylvain Bernès, Blanca Martha Cabrera-Vivas, Alejandro Durán-Hernández, Rafael Zamorano-Ulloa," *R J. Mol. Struct*, vol. 788, pp. 145–151, 2006.

[19] "Ferman A. Charvez, Marilyn M. Olmstead, Pradip K. Masharak," *Inorg. Chem.*, vol. 35, pp. 1410–1412, 1996.

[20] "Gyungse Park, Junlng Shao, Frances H. IU, Robin D. Rogers, N. Dennis Chasteen, Martin W. Brechiel, Roy P. Planalp," *Inorg. Chem.*, vol. 40, pp. 4167–4175, 2001.

[21] "Nevin Turan, Bayram Gündüz, Hanifi Körkoca, Ragıp Adigüzel, Naki Çolak, Kenan Buldurun," *j.Mex. Chem. Soc.*, vol. 58, pp. 65–75, 2014.

[22] "Samir S. Kandil, Gad B. El-Hefnawy, Eman A. Baker," *Thermochim. Acta*, vol. 414, pp. 105–113, 2004.

[23] "Nagham S. Buttrus," *Res. J. Chem. Sci.*, vol. 4, pp. 41–47, 2014.

[24] "Buttrus H. Nabeel, Saeed T. Farah," *Res. J. Chem. Sci.*, vol. 2, no. 6, pp. 43–49, 2012.

[25] "A. B. P. Lever," *Inorg. Electron. Spectrosc. 2nd Ed., Elsevier, Amsterdam*, 1985.

[26] "A.S. El-Tabl, W. Plass, A. Buchholz, M.M. Shakdofa," *J. Chem. Res.*, vol. 2009, pp. 582–587, 2009.

[27] "Halime Güzin Aslan, Servet Özcan, Nurcan Karacan," *Inorg. Chem. Commun.*, vol. 14, pp. 1550–1553, 2011.

[28] "A.W. Coats, J. P. Redfern," *Nature*, vol. 201, p. 68, 1964.